Heliyon 10 (2024) e34507

Contents lists available at ScienceDirect

Heliyon

journal homepage: www.cell.com/heliyon

Research article

Laminin 332 functionalized surface improve implant roughness and oral keratinocyte bioactivity

Sandra J. Perdomo [a,1,*], Carlos E. Fajardo [b,1], Andrés Cardona-Mendoza [a,b]

[a] Grupo de Inmunología Cellular y Molecular de la Universidad El Bosque-INMUBO, Colombia
[b] School of Dentistry, Universidad El Bosque, Bogotá, Colombia

ARTICLE INFO

Keywords:
Dental implant
Laminin 332
Oral keratinocyte
Bioactivity
Titanium surface

ABSTRACT

Objective: The biological seal (BS) at the implant-tissue interface is essential for the success of dental implants (DIs), and the absence of a proper BS can lead to peri-implantitis. The basement membrane (BM) and junctional epithelium are critical for sealing the peri-implant mucosa, and laminin 332 is an important protein in binding the epithelium to the implant surface. The aim of this study was to evaluate the response of oral keratinocytes to titanium dental implant surfaces biofunctionalized with laminin 332.

Design: The dental implant surface was treated with a piranha solution to create hydroxyl (OH) groups, facilitating biofunctionalization with laminin 332. The modified surface underwent scanning electron microscopy, surface roughness evaluation, and chemical composition analysis. Human keratinocytes from the Cal-27 line were then cultured on the modified implants for 24 and 48 h to assess viability, morphology, cytokine secretion, and mRNA expression of tissue repair-associated genes.

Results: The results showed that laminin 332 biofunctionalization of the implant surface resulted in lower values of Ra, Rq and positive surface roughness parameters Rsk, Rku and Rv. The elemental composition showed an increase in nitrogen and carbon content corresponding to protein binding. The biofunctionalized surfaces did not affect cell viability and promoted cytokine secretion (IL-1a and IL-8) and a significant increase ($p < 0.05$) in MCP-1, EGF, FGF, TGF and VEGF gene expression compared to the control.

Conclusion: In conclusion, laminin 332 coating Ti implants was shown to be effective in promoting keratinocyte adhesion, spreading, and viability. This approach could be an alternative way to improve biocompatibility.

1. Introduction

Dental implants (DIs) are currently the best prosthetic alternative for oral rehabilitation in various clinical scenarios. DIs are based on the process of osseointegration, which Brånemark defines as "The structural, functional and direct connection that is achieved only when the peri-implant mucosa heals very rapidly in the marginal region, sealing the deepest supporting structures" [1]. The interface between dental implants and soft tissue allows the formation of a biological seal (BS) that can protect the underlying structures by

* Corresponding author. Grupo de Inmunología Celular y Molecular de la Universidad El Bosque-INMUBO, Colombia.
E-mail address: perdomosandraj@unbosque.edu.co (S.J. Perdomo).
[1] These authors share first authorship.

https://doi.org/10.1016/j.heliyon.2024.e34507
Received 14 September 2023; Received in revised form 4 July 2024; Accepted 10 July 2024
Available online 14 July 2024

closing the communication between the oral microenvironment and the alveolar bone. Maintaining a BS is critical to the success of DIs, as it is the process of keratinocyte adhesion and collagen fibre insertion onto the titanium surface of the implant. In this way, the DIs are the first defence system of the peri-implant mucosa. However, the characteristics and architecture of these tissues are different from those found around the teeth, so the peri-implant tissue of the BS is weaker than that of the natural epithelium, and its integrity is more difficult to generate and maintain [2].

The deficient form of BS promotes the accumulation and colonization of biofilm in the internal peri-implant tissues, which promotes dysbiotic processes leading to pathologies such as peri-implant mucositis and peri-implantitis [3]. Furthermore, the breakdown of titanium (Ti) and its natural surface oxide and corrosion has been demonstrated to release Ti ions into nearby tissue. This release can trigger inflammatory responses and frequently result in peri-implantitis [4]. In this context, peri-implantitis is one of the biological causes of DIs failure, with consequences for the patient such as loss of alveolar bone and soft tissue [5]. Therefore, with the increasing use of dental implants for the oral rehabilitation of patients, it is necessary to develop strategies to improve the formation of BS between peri-implant tissues, especially the epithelium-tissue interface, which could be an essential factor in increasing the survival and success of dental implants [6].

The junctional epithelium plays a fundamental role in sealing the periodontal tissues from the oral environment and therefore its integrity is essential to maintain a healthy peri-implant mucosa. There is no doubt that the peri-implant tissues form a biological seal between the oral environment, the bone and the implant surface [7]. The epithelium is divided into three functional compartments: oral, sulcular and junctional, while the connective tissue is divided into superficial and deep components [8]. The basement membrane (BM) structures are similar to others and are formed by type IV collagen and laminin, the two main components. The interface by which the adherent epithelium is attached to the surface of the implant is formed by a basal lamina (BL) between the epithelium and the surface of the implant; this BL is a specialised extracellular matrix containing laminin, a protein of the matrix that mediates cell adhesion and regulates the polarisation and migration of keratinocytes, which act as anchoring plates holding the epithelial cells to the BL (Frank and Carter, 2004). The main cell adhesion protein of the BL is laminin 332, a heterotrimeric integrin-binding protein [9,10], which has been shown to be highly expressed in the cells of the inner membrane in mouse models [11,12].

In this context, both abutment material and surface topography have been demonstrated to influence soft tissue extracellular matrix deposition [13]. Several methods have been proposed to improve the quality of the soft tissue interface, including micro and macro design features of the transmucosal portion. Within these methods, the influence of material type, surface topography effect and dental implant surface modification have been evaluated [13]. Epithelial cells and gingival fibroblasts have different affinities for the adhesive proteins of the extracellular matrix; therefore, they can improve the ability of the epithelium and connective tissue components in the peri-implant mucosa to attach to implants with surface modifications. Among these, we can find surface treatments with laser anodisation [14], where the insertion of connective fibres to the implant surface is demonstrated, or the coating (functionalization) of titanium alloy with laminin-5 (now laminin 332), which has also been observed to improve the insertion of epithelial cells and hemidesmosomes in vitro [15]. Marconi et al. demonstrated that the rough surface of dual acid-etched titanium dental implants increased the expression of extracellular matrix (ECM) molecules such as fibronectin, laminin, N-cadherin, and RUNX2 in human periodontal ligament stem cells (hPDLSCs) [16]. Furthermore, Guida et al. demonstrated that the surface of oxidized implant abutments exhibited a distinct micro- and nanometer-level structure, which enhanced adhesion, proliferation, and extracellular matrix deposition by human gingival fibroblasts [17]. Considering that any change in the material of dental implants, such as structural designs and surface properties, can modulate the biological response, the functionalization of DIs with proteins from the extracellular matrix essential for the migration and adhesion of oral keratinocytes, such as laminin 332, is a promising strategy to improve the peri-implant protective conditions, which may have essential coadjuvant effects in tissue stability, improving the behaviour of long-term restorations. Therefore, the aim of this work was to modify the surface of titanium implants currently used in implant dentistry with respect to their effect on cell adhesion in order to improve implantation success and survival.

2. Materials and methods

2.1. Titanium dental implant fragments

To obtain titanium surfaces, 36 titanium dental implants (Phibo®, Avantblast® surface) were cut into fragments 3 mm long and 3.6 mm in diameter. The fragments were then ultrasonically washed in distilled water for 30 min and sterilised in an autoclave.

2.2. Cell line and culture conditions

The tongue squamous cell carcinoma cell line (CAL27) was expanded in 75 cm^2 cell culture flasks at 37 °C and grown in DMEM supplemented with 10 % bovine fetal serum (BFS) and 1 % antibiotic/antimycotic in an atmosphere of 5 % CO2 and 100 % relative humidity. The medium was changed every other day. When the monolayer reached 90 % confluence, the cells were trypsinised and used for experiments.

2.3. Biofunctionalization of the titanium surface

For the biofunctionalization of titanium surfaces, the technique described by Tack et al. (2015) was used with some modifications (Tack et al., 2015b). Briefly, to prepare the titanium surfaces, dental implant fragments were first washed with ethanol/acetone 1:1 in 40 Khz sonication for 20 min; they were then washed 3 times with sterile deionized water. After washing the dental implant fragments,

the titanium surfaces were oxidized by subjecting them to a chemical attack with "Piranha" solution (hydrogen peroxide (H2O2)/ sulfuric acid (H2SO4) concentrated 1:1) for 1 h at room temperature to generate free hydroxyl groups (Fig. 1a). At the end of oxidation, the fragments were washed twice with sterile deionized water and three times with acetone, dried at room temperature, and then at 80 °C for 15 min.

Subsequently, the silanization of the titanium surfaces was performed by the silanization liquid phase, which attempts to hydrolyze the alkoxy groups of the silane to the resulting silanol groups, which join with the hydroxyl groups present on the titanium surface (previously oxidized). For this purpose, titanium fragments were immersed in APTES (3-aminopropyl triethoxysilane - Sigma-Aldrich) solution 5 % in toluene (Sigma-Aldrich) at 120 °C for 3 h in a reflux condenser system (Fig. 1b). The implant fragments were then washed twice with pure toluene for 20 min under sonication with deionized distilled water. Finally, the implant fragments were hardened at 105 °C for 10 min, threatened with 5 % glutaraldehyde (GA) for 1 h, and washed three times with deionized distilled water. In this step, the APTES condensation results in siloxane oligomers that react to form branched siloxane bonds (-Si-O-Si-) or a chain of polymerized silanes that when contacted with hydroxyl groups present on the surface of titanium form very stable -Si-O-metal bonds. The siloxane groups are covalently bonded to the OH- groups present in the titanium (Fig. 1c). Finally, for the various experiments, the implant fragments were immersed in bovine serum albumin (BSA) at 10 mg/ml or in laminin 332 at 10 ng/ml (Fig. 1d).

2.4. Cell viability and epithelial adhesion to laminin 332 functionalized titanium surfaces

Adhesion assays of Cal-27 epithelial cells to the functionalized titanium surfaces were performed in 96-well plates at a cell density of 50,000 cells/well. In these experiments, cells were co-cultured with the titanium implants with and without surface coating (n = 3 for each group) for 4, 24, and 48 h. At the end of each time period, non-adherent cells were washed with PBS. The implant fragments were then transferred to U-bottomed 96-well plates, and the cells adhering to the titanium surfaces (with or without functionalization) were separated by enzymatic treatment with 50 μL trypsin-EDTA (Sigma Aldrich) for 5 min and then stained with 100 μL DNA Hoechst at 33342 2.5 μg/ml and calcein-AM (Thermo Fisher Scientific, MA, USA) for 10 min (Thermo Fisher Scientific, MA, EE. UU). After staining, the cells were centrifuged to remove the staining residue, washed and resuspended in PBS, and finally observed under a Zeiss fluorescence microscope (Carl Zeiss Microscopy, Jena, Germany). This procedure allows the identification of live cells when incubated in the presence of calcein-AM modified by the metabolism of intracellular esterases.

2.5. Characterization of titanium surfaces by scanning electron microscopy (SEM)

The implant fragments functionalized and/or co-cultured with CAL-27 cells were dried in a critical point (Samdri-795. Tousimis), coated with gold to be analyzed, and characterized by scanning electron microscopy (SEM; SEM JSM-IT100 Jeol, Tokyo, Japan). The different modifications of the surfaces were evaluated: control without treatment, treated surfaces up to GA, and surfaces with laminin

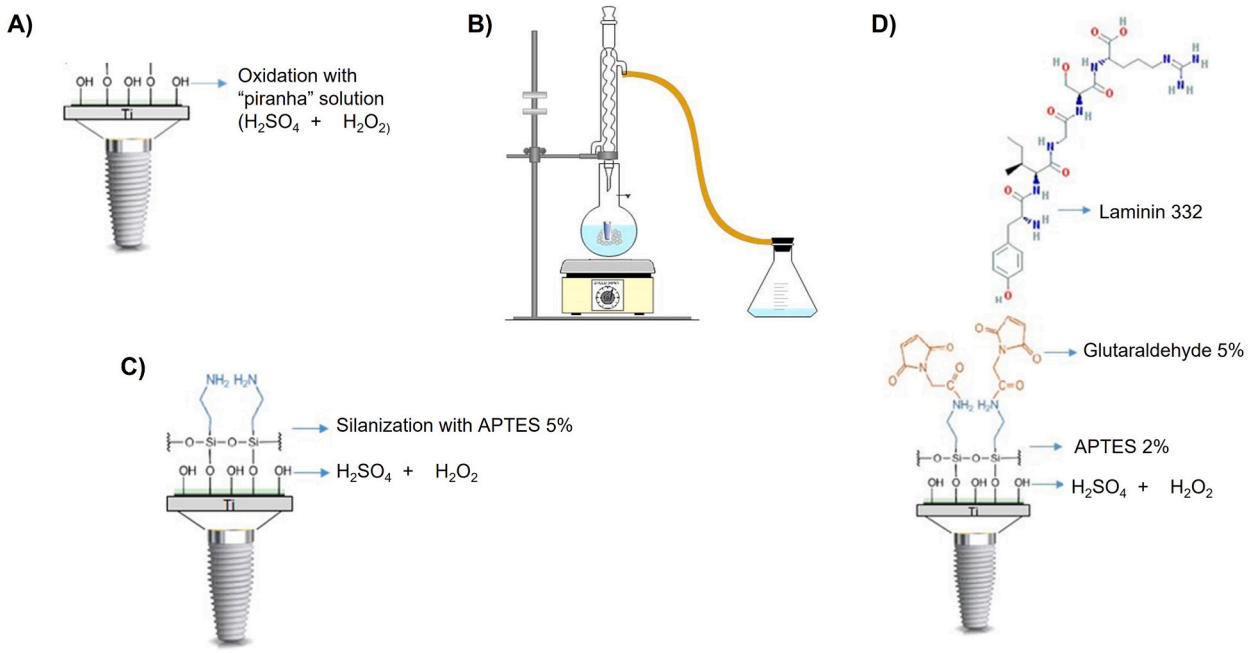

Fig. 1. Schematic representation of the biofunctionalization process of titanium surfaces (dental implant fragments). A) Chemical attack with piranha solution and generation of hydroxyl groups performed on titanium dental implant fragments. B) Condensor reflux system for C) Silation of titanium dental implant fragments with (3-aminopropyl) triethoxysilane (Aptetes) to 5 %. D) Complete biofunctionalization of titanium dental implant fragments with Laminin 332.

332. Energy dispersive X-ray spectroscopy (EDS) was used to analyze the elemental composition of the surface.

2.6. Characterization of titanium surface topography

The roughness of titanium implants was measured on images obtained by SEM using the surfcharj.class plugin of ImageJ, both for untreated surfaces and for the surface treated with the "Piranha" solution and functionalized with protein (albumin or laminin 332). The roughness parameters of 6 implants of each group were calculated according to the ISO 4287/2000 standard. The mean roughness (Ra) was analyzed, and the mean square root of roughness (Rq), evaluated profile kurtosis (Rku), evaluated profile skew (Rsk), lower valley (RV), highest peak (Rp), and total profile height (Rt) were obtained. The main parameters used to define the roughness were:

- Ra (arithmetic mean of the profile deviations): The arithmetic mean of the absolute value of the distance from the center line to the R(YI) profile within the sample length. Ra is calculated in NM and is the parameter usually chosen to quantify the roughness of a surface in general; it is given by formula (a):

$$Ra = \frac{1}{a_z} \int_0^{a_z} |y(x) - m| \mathrm{d}x \quad \text{a}$$

-Rq (average of the square root of the profile deviations): It is the average value of the square root of the deviations of the profile with respect to the center line within the sample length. Due to the quadratic operation, this parameter is more sensitive than Ra to the extreme values. RQ has a statistical meaning as it is associated with the standard deviation of the distribution of the profile heights and is given by formula 2 (b):

$$Rq = \sqrt{\frac{1}{l} \int_0^{l} Z^2(x) \mathrm{d}x} \quad \text{b}$$

2.7. Measurement of soluble cytokines and chemokines produced by epithelial cells adhering to titanium surfaces functionalized with laminin 332

Culture supernatants at 4, 24, and 48 h were collected, centrifuged at 500×*g* for 5 min, and frozen at −80 °C until analysis. Soluble levels of proinflammatory cytokines (IL-1β, IL-1α, IL-6, TNF-A) and chemokines (IL-8, RANTES, MCP-1, MIP-1) were measured by flow cytometry using the LEGENDdplex ™ Kit (Biolegend, USA) according to the manufacturer's instructions. Data acquisition was performed on the BD FACS Accuri ™ C6 Plus and data were processed in the LEGENDdplex software. Three independent experiments were performed for each time point.

2.8. Analysis of the expression of genes associated with the tissue repair process in oral keratinocytes adhered to biofunctionalized titanium surfaces

Expression of genes associated with the tissue repair process: EGF, VEGF, TGF-β and FGF in oral keratinocytes (CAL-27) adhered to the biofunctionalized titanium surfaces were evaluated by qRT-PCR. Samples from 4, 24, and 48 h cultures were immersed in 400 μL lysis buffer (Zymo Research Corp, USA) and stored at −80 °C until analysis. The Quick-RNA ™ miniprep kit (Zymo Research, USA) was used for RNA extraction according to the manufacturer's specifications. The RNA obtained was quantified using a Nanodrop spectrophotometer (Thermo Fischer Scientific) at 260/280 nm. Samples were adjusted to 10 ng/ul for all experiments. For qRT-PCR, the Luna® Universal One-Step RT-QPCR Kit (New England Biolabs-NEB) was used, and signal detection was performed in Bio-rad CFX96 (Bio-Rad, USA) using the following primers: TGFB forward 5′-AAGTTCAGAGCAGAGTACAC-3′, reverse 5′-TATCGCCAGGAATTGTTG-3'; GAPDH forward 5′GAAGGTGAAGGGTCGGAGTC-3′, reverse 5′-GAAGATGGTGATGGGATTTC-3′; FGF2 forward 5 ′-gcattcacaccactacaa-3′, reverse 5′-caactcgtaacatccat-3′; EGF forward 5 ′GGACCACCTGATGAATATC-3′, reverse 5 ′-CCATAACCATCTGCTCTG-3′; VEGF forward 5 ′-AATGAAGGAGAGAGGAGAGACT- 3′, reverse 5 ′GGTGATTTAGCAGCAGCAGCAGA-3′. PCR amplification consisted of an initial retrotranscription step at 55 °C for 10 min, followed by a denaturation step at 95 °C for 10 min, 40 cycles of PCR at 95 °C for 15 s and 60 °C for 60 s. The relative expression of each gene was normalized to GAPDH using the 2-ΔΔCT relative quantification Pfaffl formula. Efficiency was calculated using LinRegPCR. Three independent experiments were performed for each time point.

2.9. Statistical analysis

All quantitative measurements were performed in triplicate and each data point represents the mean ± (standard deviation). Statistical significance between the control and experimental groups was determined using a two-tailed unpaired *t*-test with unequal variance. In addition, the data involving more than two groups were analyzed using unidirectional ANOVA and the Q post hoc test. Significance levels were set at $p < 0.1$ and $p < 0.05$.

3. Results

3.1. Physicochemical characterization of the surfaces during the biofunctionalization process

3.1.1. Surface roughness analysis

The roughness of titanium surfaces after Piranha treatment is a physical property that influences surface-molecule and cell-cell interactions. Therefore, it was evaluated if the Piranha solution treatment affects the roughness of the titanium surfaces of the implant fragments and if these changes may or may not affect the functionalization of proteins and the cellular response. The images and values of the roughness parameters of the Piranha-treated titanium surfaces were obtained by scanning electron microscopy using the ImageJ plugin Surfcharj.class Plugin program (Fig. 2A–F). The measurement of R values across the surface provides roughness values according to the ISO 4287/2000 standard. The following amplitude parameters were selected for the roughness analysis of the titanium implant surface: Ra, Rt, Rq and Rku.

It was observed that the surfaces treated with Piranha solution suffered significant surface modifications, as evidenced by a different texture and roughness compared to the control (no treatment) (Fig. 2A–F). The roughness measurements (Fig. 2G–H) showed that the Ra and Rq values were significantly higher ($p < 0.05$) in the samples treated with piranha solution compared to the control samples of the commercial implant PHIBO® Avantblast® surface. This value indicates that the chemical attack of the Piranha solution causes an erosion that modifies the morphology and the titanium surface. In addition, negative values for Rsk, Rsu and Rv were observed in the treated implants compared to the control; these negative values indicate that the treated surfaces are formed by valleys, while the untreated surface contains mainly peaks and roughness. It should be noted that a negatively biased surface is suitable for lubrication. The roughness in the Piranha solution treated samples could provide a homogeneous silane and protein distribution. Due to the higher roughness, the superficial area index (SAI) of the Piranha solution treated samples was higher than that of the control samples, which may affect the amount of immobilized biomolecules on the titanium surface and consequently the cellular response.

Subsequently, the samples treated with APTES and GA (Ti + APTES + GA) were analyzed after the chemical attack with the Piranha solution. In Fig. 3A–F, it is observed that the surface of the surfaces functionalized with laminin 332 (Ti + APTES + GA + laminin 332) suffers modifications generated by the treatment and adhesion of the protein (Fig. 3B–D), compared to the control surfaces (Fig. 3A, C, E). In addition, in the samples functionalized with the protein, the value of Ra was similar to that found in the samples treated with Piranha solution; however, the value of Rq did not show any changes. The Ra and Rq values of the surfaces functionalized with laminin 332 (Ti + APTES + GA + laminin 332) were lower than those of the surfaces treated with GA (Ti + APTES + GA) and those of the surfaces treated only with Piranha solution ($p < 0.05$) (Fig. 3G–H). In addition, negative RSK, RKU and RV values were observed on the

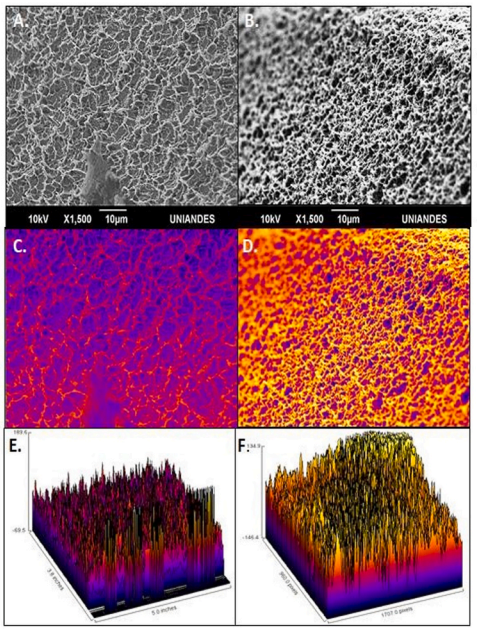

G)

Sample/ Parameter	Rq (nm)	Ra (nm)	Rsk	Rku	Rv	Rp	Rt	Rc
Piranha solution	39,94 ± 3,5	69,97 ± 3,9	- 0,21 ± 0,007	- 0,52 ± 0,02	- 91,16 ± 0,7	245,92 ± 2,8	237 ± 7,1	12,83 ± 0,15
Ti. Control	16,17 ± 1,1	12,63 ± 0,9	0,22 ± 0,001	0,65 ± 0,13	62,83 ± 5,5	183,59 ± 9,7	128,5 ± 7,7	124,5 ± 2,5

H)

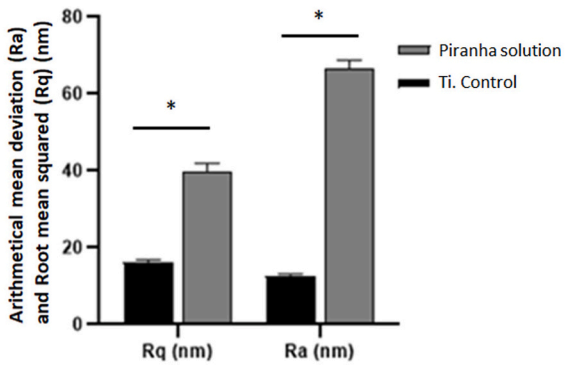

Fig. 2. Roughness evaluation of titanium surfaces (dental implant fragments) after chemical attack with Piranha solution. A) Sweep microscopy microphotography (X1,500) of the dental implant without treatment (control). B) Sweep microscopy microphotography (X1,500) of the dental implant treated with Piranha solution. Images of gradients of the topography of the surfaces of dental implants C) control and D) treated with Piranha solution. Three-dimensional profiles representative of the surfaces of dental implants E) control and F) treated with Piranha solution. G) Values of the roughness parameters determined on the surfaces of dental implants control and after treatment with Piranha solution. H) Comparison of Ra and Rq roughness parameters on the surface of control dental implants and surface treated with Piranha solution. * ($p < 0.05$) Control vs. Piranha Solution.

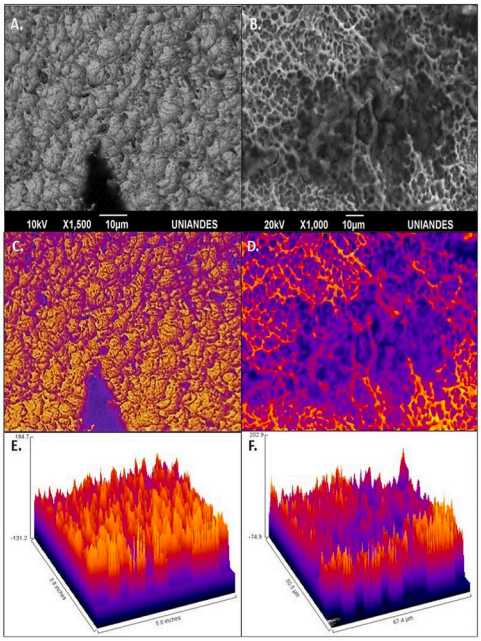

G)

Sample/ Paremeter	Rq (nm)	Ra (nm)	Rsk	Rku	Rv	Rp	Rt	Rc
Ti+APTES+GA +Laminin 332	19,26 ± 3,2	16,10 ± 1,5	0,35 ± 0,6	0,93 ± 0,78	-33,4 ± 2,3	41,10 ± 1,6	74,52 ± 0,3	0,19 ± 0,9
Ti + APTES + GA	33,18 ± 2,6	27,07 ± 2,9	- 0,007 ± 0,1	- 0,40 ± 0,12	7,93 ± 1,6	232,4 ± 3,8	224,4 ± 0,3	111,0 ± 0,5
Piranha solution	39,94 ± 3,5	69,97 ± 3,9	- 0,21 ± 0,007	- 0,52 ± 0,02	- 91,16 ± 0,7	245,92 ± 2,8	237 ± 7,1	12,83 ± 0,15

H)

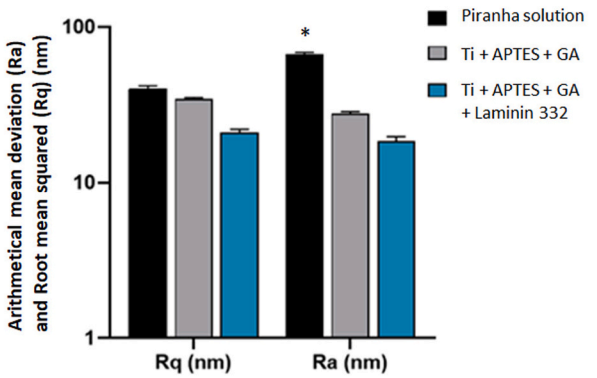

Fig. 3. Roughness evaluation of titanium surfaces (dental implant fragments) biofunctionalized with laminal 332. A) Sweep microscopy microphotography (X1,500) of the dental implant treated up to the glutaraldehyde step. B) Sweep microscopy microphotography (X1,500) of the dental implant biofunctionalized with laminal 332. Gradient images of the topography of dental implant surfaces C) treated up to the glutaraldehyde step (Ti + APTES + GA) and D) biofunctionalized with laminin 332. Representative three-dimensional profiles of dental implant surfaces E) treated up to the glutaraldehyde step (Ti + APTES + GA) and F) biofunctionalized with laminin 332. H) Comparison of Ra and Rq roughness parameters on the surface of dental implants before and after biofunctionalization with Laminin 332. *($p < 0.05$) Piranha solution vs. surface treated with glutaraldehyde vs. surface functionalized with Laminin 332.

surfaces treated with Piranha and GA solution (TI + APTES + GA), indicating that the surface retains the morphology and roughness patterns formed by the surface valleys. In contrast, surfaces functionalized with Laminin 332 (Ti + APTES + GA + Laminin 332) showed positive values ($p < 0.05$). The increase in these values on the surface with the protein suggests a larger contact area, which probably favors cell adhesion (Fig. 3B, D, F).

3.1.2. Surface analysis by scanning electron microscopy - energy dispersive X-ray spectroscopy

Energy-dispersive X-ray spectroscopy (EDS) was used to analyze the chemical element composition of the surfaces of the implant fragments in the different study conditions. The untreated titanium surfaces (control) showed high levels of carbon (80.42 %) and oxygen (3.19 %) and low levels of titanium (1.79 %) (Fig. 4A and C). This low titanium content is explained by the 3–7 nm titanium dioxide layer covering the implant. The high carbon content of the untreated surface suggests contamination with "normal" organic hydrocarbons, which inevitably occurs when titanium is exposed to the air. To remove these environmental contaminants, the implant fragments were first cleaned with an ethanol/acetone mixture prior to chemical attack with Piranha solution. The surfaces treated with Piranha solution showed an increase in the percentage of titanium (48.75 %), oxygen (7.23 %), nitrogen (1.2 %) and a decrease in the percentage of carbon (45.52 %) compared to the control samples (Fig. 4A and C). The increase in oxygen with the Piranha solution indicates the formation of hydroxyl (OH) groups, which are necessary to form bonds with the silane.

The fragments of the implants in the following coating stages were also evaluated by SEM and EDS. In the first step of the covalent coupling process, it was observed that the titanium surface treated with IT + APTES + GA had a higher silicon content (8 %), nitrogen content (4.5 %) and titanium content (20.6 %) than the control surfaces (untreated). The silicon content on the treated surface (Ti + APTES + GA) is due to APTES (Fig. 4B and D). Laminin 332 was covalently coupled to the glutaraldehyde linker in the functionalization step; in these samples, an increase in carbon content (64.08 %) and nitrogen (18.55 %) was detected, due to the carboxyl and amino groups contained in the protein, compared to the samples treated up to Ti + APTES + GA (Fig. 4D).

3.2. Effect of functionalizing titanium surfaces with laminin 332 on the viability, morphology and cellular response of oral keratinocytes

3.2.1. Functionalized titanium surfaces do not affect cell viability

To evaluate whether the treated and functionalized titanium surfaces exerted a cytotoxic effect on adherent oral keratinocytes (CAL-27), the cells were co-cultured with fragments of functionalized implants for 4, 24, and 48 h, the surfaces were washed with PBS, and the adherent cells were harvested with trypsin-EDTA and labeled with calcein-AM and Hoechst 33342 to perform cell viability

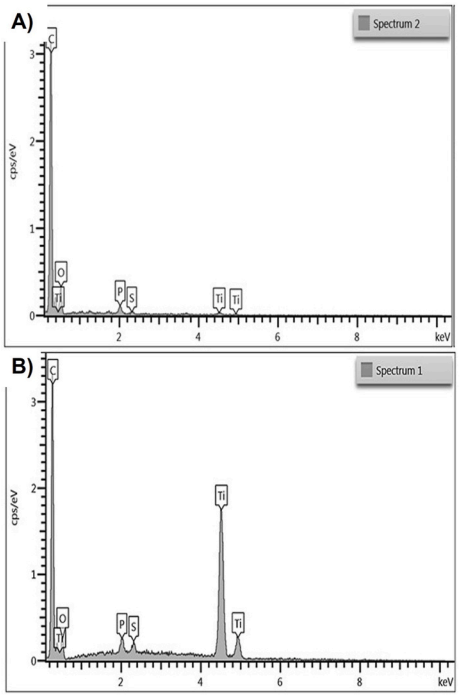

C)

Element	Ti [%]	C [%]	N [%)]	O [%]
Piranha solution	48,75	45,52	1,2	7,23
Ti. Control	1,79	80,42	0,5	3,19

D)

Element	Ti [%]	C [%]	N [%]	O [%]	Si [%]
Ti. Control	1,79	80,42	0,5	16,19	-
Ti + APTES + GA	20,6	27,64	4,5	19,36	8
Ti + APTES + GA + Laminin 332	1,24	64,08	18,55	14,32	-

Fig. 4. Analysis of the chemical composition by EDS of titanium surfaces (dental implant fragments) after chemical attack with piranha solution and biofunctionalization with laminin 332. a) Dental implant without treatment (control). B) Dental implant treated with Piranha solution. C) and D) Percentage composition of chemical elements of the implant surfaces in the different conditions evaluated.

tests by fluorescence microscopy. As shown in Fig. 5A–C, a good adherent cell density was obtained from the functionalized surfaces at the different co-culture times. In addition, the adhered cells remained viable under these conditions, as shown by calcein-AM staining (Fig. 5D–F). The complementary analyses show that the adherent cells release up to 10 % LDH at 48 h of co-culture, which is statistically significant with respect to 24 and 48 h $p \leq 0.001$ (Fig. 5G), maintaining the viability of 99.76 ± 0.06 % at 4 h, 94.87 ± 1.53 % at 24 h, and 90.18 ± 0.6 % for the 48 h of co-culture $p \leq 0.001$ (Fig. 5H). Therefore, we can conclude that treated and functionalized titanium surfaces do not induce a significant cytotoxic effect on oral keratinocytes Cal-27.

3.2.2. Changes in the morphology of oral keratinocytes on surfaces functionalized with laminin 332

SEM images showed that cells adhered to both the control surfaces (Fig. 6B) and the treated surfaces (Ti + APTES + GA) (Fig. 6D) or functionalized surfaces (Ti + APTES + GA + laminin 332) (Fig. 6E–F). Morphologically, cells on the control surfaces (Fig. 6B) showed mainly an elongated shape, whereas cells on the functionalized surfaces were observed with a network of very fine cell extensions, which help their fixation on the locally smooth surface where protein is found (Fig. 6E–F). Cell-cell contacts were also visible on all surfaces after 4 days of culture (Fig. 6). Cells showed a relatively elongated and flattened morphology in the treated implants (TI + APTES + GA) (Fig. 6D). No variability in cell morphology was observed between different implants of the same group. On the other hand, roughness seems to influence the extension and morphology of cells on different surfaces. In addition, a higher number of adherent cells are observed on the protein-functionalized surfaces (Fig. 6F).

3.2.3. Levels of MCP-1, IL-α, and IL-8 are increased in cultured cells on laminin 332 functionalized surfaces

The production of cytokines is one of the primary cellular responses to any stimulus and to the microenvironment in which the cells are located. To measure and analyze the cytokine profile of oral keratinocytes on the titanium surfaces, the 24- and 48-h cell coculture (cell-implant) supernatants were collected and the cytokine solubility was measured by flow cytometry.

The cytokine levels were very similar between the surfaces; however, the laminin 332 functionalized surface induced higher levels of the proinflammatory cytokine IL-1α ($p < 0.05$) and of the chemokines MCP-1 ($p < 0.05$) and IL-8 ($p < 0.05$) at 24 h of culture compared to the control surfaces (Fig. 7A and C). After 48 h of co-culture, the high levels of MCP-1 were significantly maintained compared to the control ($p < 0.05$); however, the levels of IL-1α and IL-8 decreased slightly compared to 24 h of cultivation, although the levels of these cytokines were maintained higher than the control (Fig. 7B and D).

3.2.4. Functionalization of titanium surfaces with laminin 332 induces increased gene expression of TGFβ-1 and growth factors

The activity of TGFβ-1 and growth factors is crucial for promoting tissue repair and regeneration processes (Abarca-Buis et al., 2021). Therefore, gene expression of TGFβ-1, vascular endothelial growth factor (VEGF), fibroblast growth factor (FGF), and epidermal growth factor (EGF) in oral keratinocytes was determined by real-time PCR after 24 and 48 h of co-culture (implant-cell).

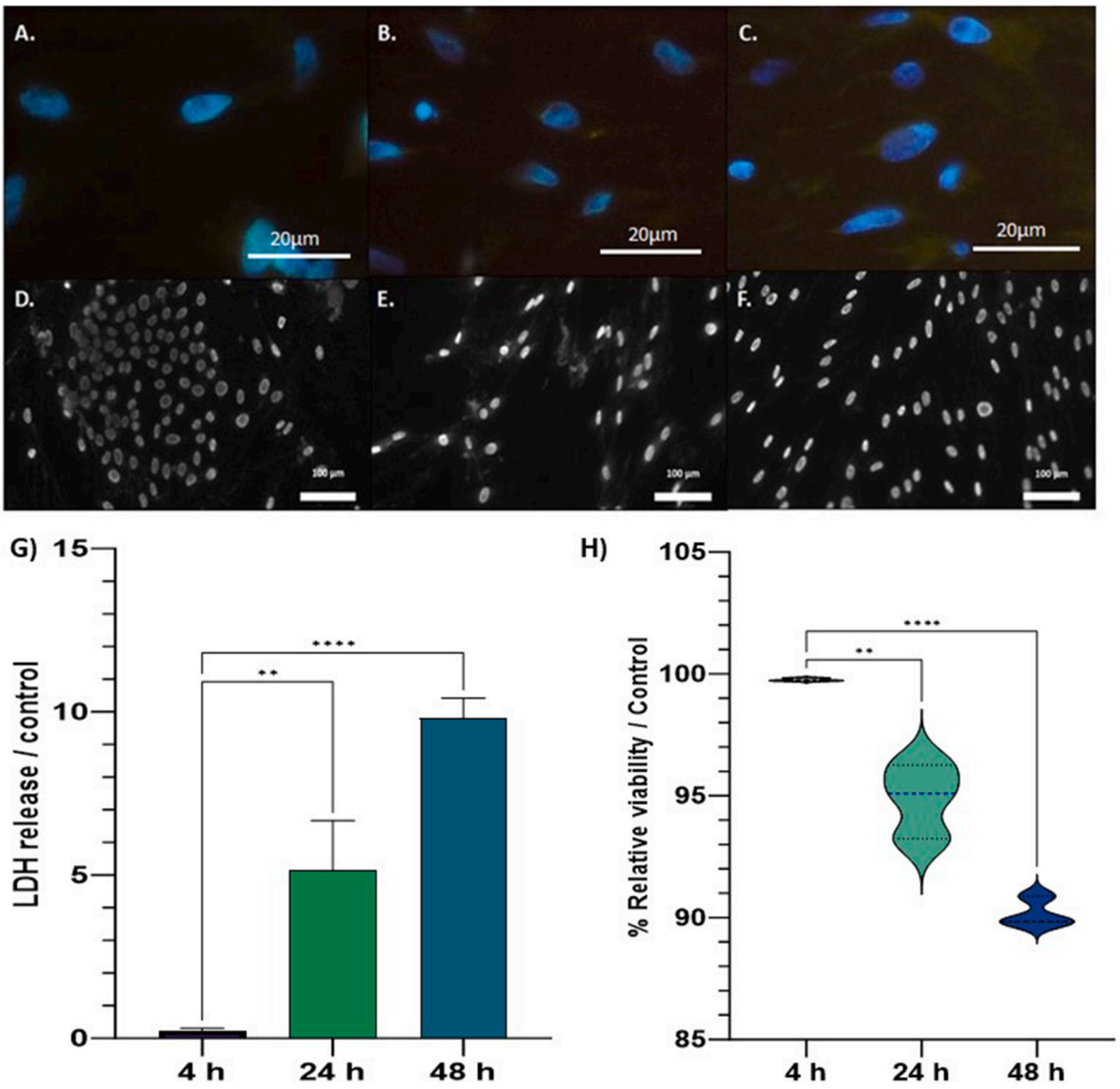

Fig. 5. Cell viability assay and fluorescence microscopy of Cal-27 cells on titanium surfaces (dental implant fragments) functionalized with laminin 332. Cells were enzymatically harvested from dental implants A-D) without treatment (control) and after B-E) 24 h and C–F) 48 h of seeding and then labeled with calcein-AM and Hoechst 33342 to observe their viability (A, B, C) or observed in the dark field (D, E, F). Cell viability was measured by G) the percentage of lactate dehydrogenase (LDH) released into the supernatant of the culture medium *** ($p < 0.001$) and by H) the percentage of viability relative to the control*** ($p < 0.001$). All data are presented as mean ± SEM of three independent implants.

The results were normalized to the expression levels of the endogenous reference gene GAPDH and are presented as relative expression compared to cells seeded on control surfaces (no treatment). Interestingly, the surfaces functionalized with laminin 332 induced a significant increase ($p < 0.05$) in the gene expression of TGFβ-1 (Fig. 8A), FGF (Fig. 8B), EGF (Fig. 8C), VEGF (Fig. 8D) compared to the control. The increase in the expression of these genes can be considered significant since it is more than 100-fold, indicating that laminin 332 adhered to the titanium surface promotes repair/regeneration of the tissue profile in oral keratinocytes.

4. Discussion

The soft tissue barrier around a dental implant plays a critical role in the success of dental implants by protecting the underlying hard tissue structures and providing a BS that prevents complications associated with infection. Inflammatory infiltrates due to bacterial colonization at the implant interface can cause epithelial down growth and subsequent peri-implant bone loss [18]. In natural

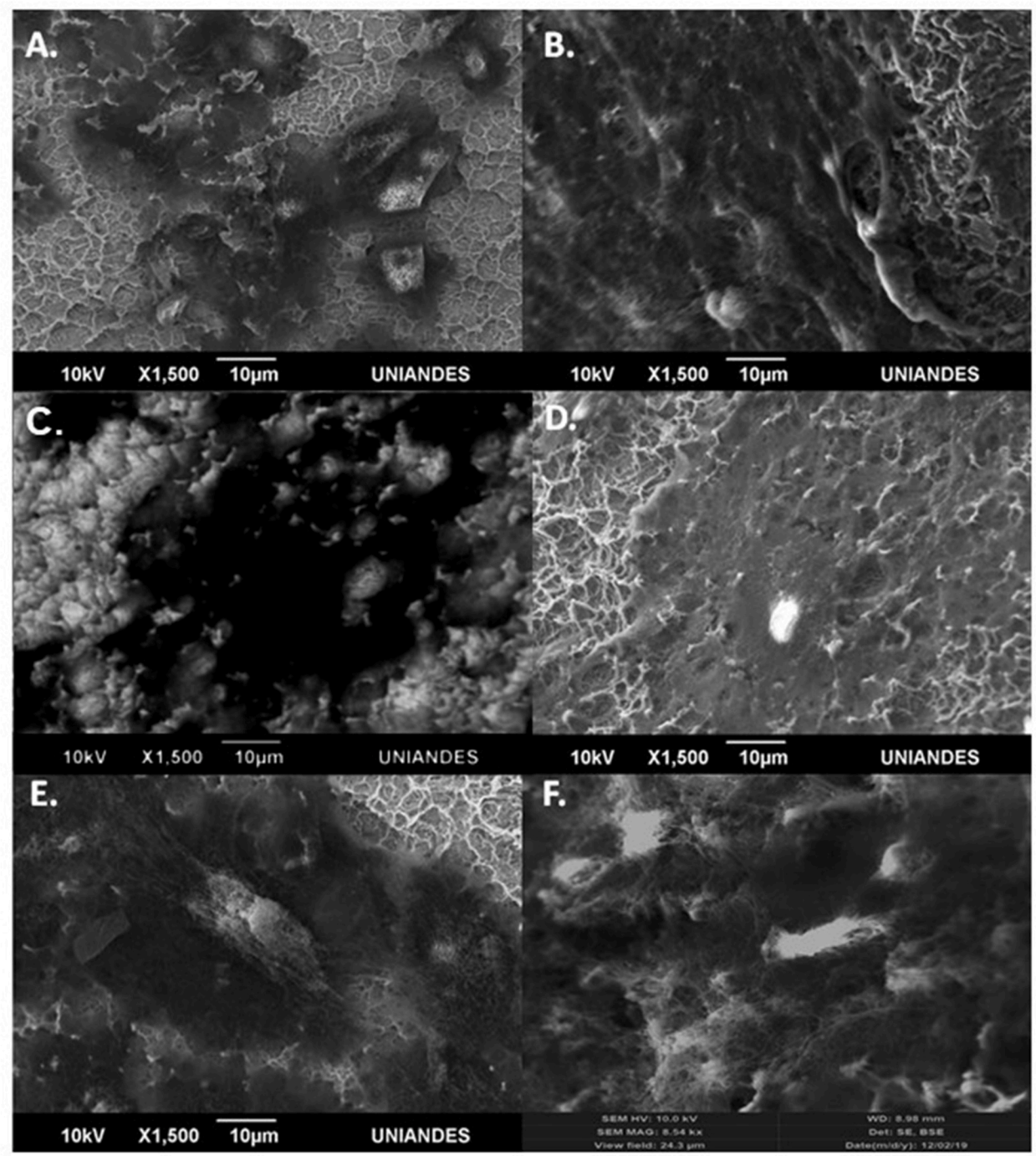

Fig. 6. SEM images of oral keratinocytes (CAL-27) adhered to A-B) untreated dental implants (control); C-D) dental implants coated with APTES + glutaraldehyde; E-F) biofunctionalized dental implants with laminin 332 after 24 h of culture.

teeth, the soft tissues adhere firmly to the enamel and cementum on the tooth surface, providing a solid defense for the alveolar bone [19]. To improve this BS around dental implants, several implant surface modification procedures have been introduced to improve bone-implant contact, but little research has been conducted on peri-implant soft tissue sealing. However, peri-implant soft tissues are becoming increasingly important as providers of BS and long-term implant stability. Therefore, the characteristics of any surface modification and the physicochemical properties at the level of dental implants can influence cell adhesion and improve their ability to promote and accelerate the healing and restoration processes of soft tissues after implantation.

Considering the need to find new alternatives to improve biological sealing processes, this work aimed to evaluate the response of

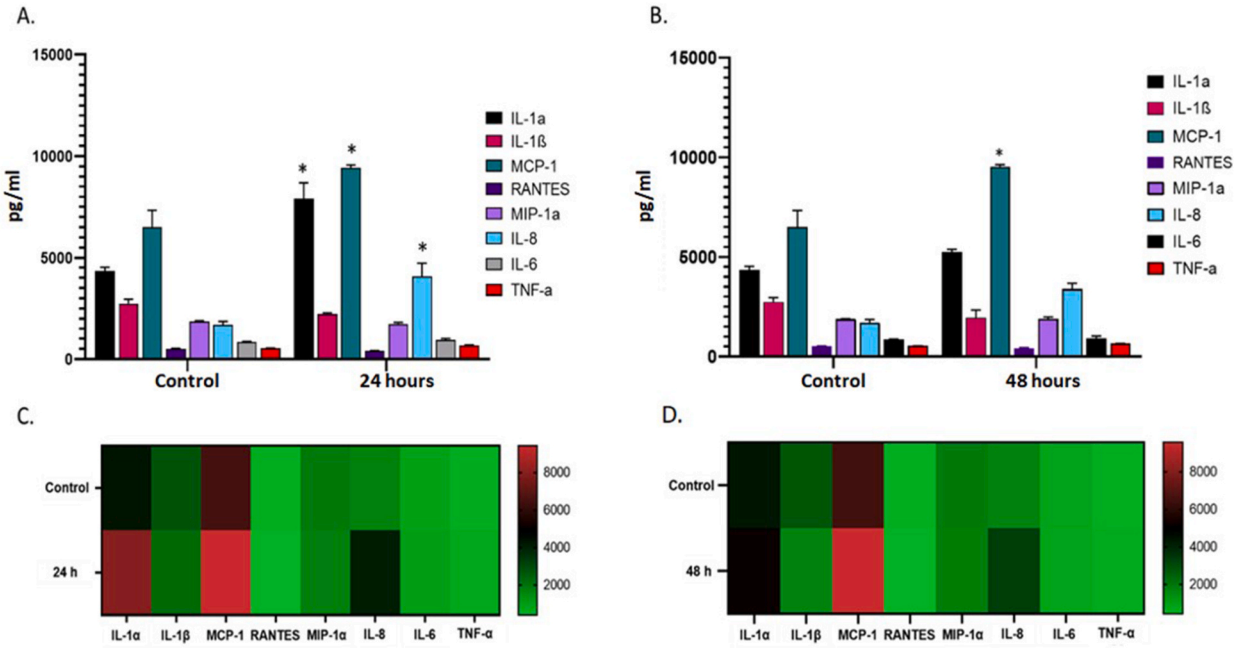

Fig. 7. Soluble cytokine levels produced by Cal-27 cells cultured for 24 and 48 h on dental implants (implant fragments) biofunctionalized with laminin 332. A) Soluble proinflammatory cytokine levels produced by Cal-27 cells cultured for 24 h on dental implants without treatment (control) and biofunctionalized with laminin 332. B) Soluble proinflammatory cytokine levels produced by Cal-27 cells cultured for 48 h in dental implants without treatment (control) and biofunctionalized with laminin 332. * ($p < 0.05$) compared with control. C) Heat map showing the average values of cytokine concentrations in the supernatants of CAL-27 cells cultured on dental implants for 24 h and D) 48 h. For each cytokine, the values were normalized and transformed into color codes representing higher (red), intermediate (black), or lower (green) concentrations.

oral keratinocytes to biofunctionalized titanium dental implant surfaces with laminin 332. This protein is a critical molecule in mucosal wound healing and the formation of mucosal seals in the junctional epithelium of the gingiva. It has been reported to be an excellent promoter of gingival epithelial cell adhesion [12,20].

The biofunctionalization of surfaces is a process that includes physicochemical treatments aimed at obtaining the immobilization of bioactive molecules such as laminin 332. In this regard, the chemical attack with piranha solution (sulfuric acid and hydrogen peroxide) has been used in several studies as a pre-silanization treatment [21], both to clean organic residues and as a strategy to hydroxylate the surface and make it highly hydrophilic for functionalization purposes [21,22], in addition to modulating the interactions on the titanium surface and the surrounding tissues. Finally, APTES as a silanization mechanism to form covalent bonds exposing amino groups on the titanium surface and allowing the coupling of proteins has been a good strategy for the biofunctionalization of these surfaces.

The increase in roughness observed in this study due to the chemical attack by the piranha solution caused an erosion of the titanium surface, changing both morphology and area (Fig. 2), similar to other studies in which they have observed changes in the roughness of the titanium surface using chemical attacks with hydrogen peroxide solutions [23,24].

In order to adequately compare the nanoarchitecture of the treated surfaces, the roughness parameters Ra and Rq were used to measure the surface at the nanometer scale [25] and to define whether the generated modification has a significant effect on the degree of cell attachment. Interestingly, in the first steps of modification of the titanium surface, the chemical attack with piranha solution showed the highest values of Rq and Ra, suggesting the generation of an irregular surface that could influence the number of immobilized biomolecules on the surface and consequently have an effect on the cellular response. This behavior has been demonstrated in other studies, where the increase in surface roughness, achieved by grinding or spraying with titanium plasma, resulted in a better mechanical establishment of the implant due to bone growth in the cavities [26] and an increase in the contact surface, which translates into a greater cell adhesion capacity [27]. On the other hand, negative values of Rsk found in Piranha solution treatment have been associated with porous surfaces with deep valley morphology, while negative Rku describes porous surfaces with peak and valley morphology [28].

In addition, when comparing the piranha-treated and laminin 332 biofunctionalized surfaces, there were significant differences in topography, with a measurable decrease in surface roughness Rq after protein immobilization from 39.94 ± 3.5 to 19.26 ± 3.2 nm (Fig. 3). Laminin 332 is a large protein composed of 3 separate chains with a total molar mass of 810 kDa [29], which occupies an area and volume on surfaces [30], and also tends to form polymerized structures, further increasing its relative size. These properties of the immobilized protein, as well as the texture characteristics, have a significant impact on the immobilization efficiency [31].

In this sense, it has been described that increasing the roughness creates a larger contact surface, increases the surface energy, and

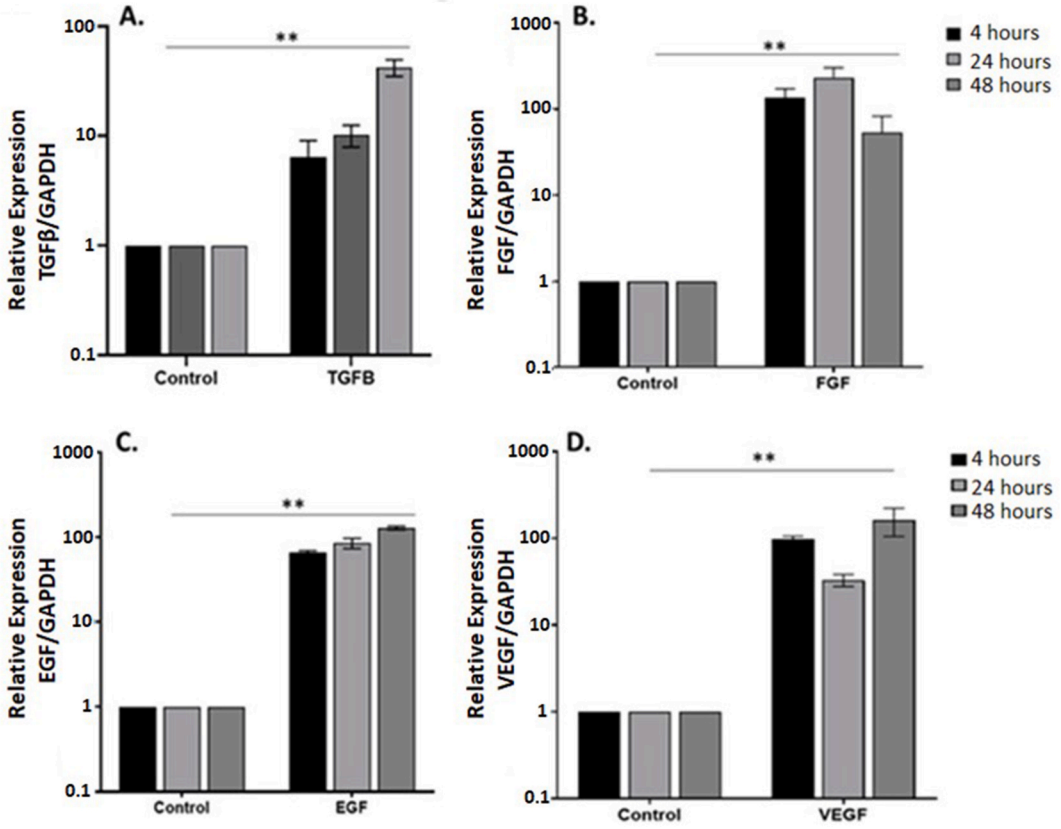

Fig. 8. Expression of tissular repair/healing genes in Cal-27 cells cultured for 4, 24, and 48 h on dental implants (implant fragments) biofunctionalized with laminin 332 evaluated by RT-qPCR. A) Transforming Growth Factor-β (TGF-β) gene. B) Fibroblast Growth Factor (FGF) gene. C) Epidermal growth factor (EGF) gene. D) Vascular endothelial growth factor (VEGF) gene. ** ($p < 0.05$) compared with control. Housekeeping GAPDH gene.

improves the wettability of the surfaces; for this reason, it was decided to use piranha solution, since the treatment with hydrogen peroxide increases the biocompatibility, bioactivity, and conductivity on the bone [27]. Similarly, the surface treatment increased the Ti content before and after by 1.79 %–48.75 %, respectively. This indicated an increase in the TiO2 layer.

In addition to surface topography, the integration of an implant can be significantly influenced by bioactive protein coatings [32, 33]. Laminin 332, a bioactive protein, can promote epithelial cell adhesion through interactions mediated by RGD motifs and can induce an increase in extracellular matrix deposition by stimulating the migration and adhesion of these cells [34], in part by proportionally increasing the number of active sites for the bioactive molecules and cells.

One of the main reasons for using Piranha solution treatments is to eliminate contaminants that may be present on the surface, which can ultimately reduce the capacity and efficiency of subsequent functionalization steps, such as silanization with APTES and protein immobilization. Therefore, it is important to determine the chemical elements present on the surface after treatment with Piranha solutions and before immobilizing the protein on the titanium surface. In this work, after treatments with piranha solution, a significant decrease in the percentage of carbon peak was observed (control: 80.42 % vs. piranha: 45.52 %) (Fig. 4C) and a significant increase in the peak percentages of titanium (control: 1.79 % vs. piranha: 48.75 %), as well as oxygen (3.19–7.23 %), indicating that this treatment can reduce surface contamination and impurities. Baranowski et al. [35] used piranha solution to treat titanium disks and then biofunctionalized them with bone sialoprotein to improve osseointegration at the bone-implant interface and reduce osseointegration micromovement and loosening. Similar to our results, they observed an increase in titanium and oxygen content after treatment with the Piranha solution.

In addition to the reduction of impurities, the Piranha solution was used to oxidize the titanium surface and increase the concentration of hydroxyl groups, which favors a more significant number of bonds with the APTES [36]. In this sense, an increase in the percentage of the oxygen peak (control: 3.19 % vs. piranha: 7.23 %) was observed after treatment with the piranha solution (Fig. 4C). In addition, the titanium-carbon-oxygen concentrations were significantly modified in the different stages of biofunctionalization. Furthermore, a significant increase in nitrogen concentration was observed after immobilization of laminin 332 (control: 0.5 % vs. (IT + APTES + GA + laminin 332): 18.55 %), coinciding with an increase in carbon content (compared to the surfaces treated with glutaraldehyde) (Fig. 4D), due to the carbon backbone and nitrogen groups contained in laminin 332.

Several studies have shown that laminin 332 is an extracellular protein closely associated with epithelial cell adhesion and

migration through binding to integrin α6β4 and hemidesmosome formation [37,38]. In this study, the biofunctionalization process with Laminin 332, at 4, 24 and 48 h of co-culture, has no significant cytotoxic effects on the cells, since the maximum reduction in cell viability was 10 % at 48 h (Fig. 5H), which is deepened by fluorescence microscopy of the cells recovered from the biofunctional surfaces (Fig. 5A–C). The results are similar to other studies such as Tack et al. [23], where mesenchymal cells on biofunctionalized titanium showed a mortality rate of only 2 %. One interesting finding in the present study was that the modification of dental implant surfaces with laminin 332 increased the cell adhesion.

All healing processes involve different phases: hemostasis, inflammation, cell proliferation, and regeneration. These phases are regulated by different cells, cytokines and growth factors. In this study, the effect of the biofunctionalized titanium surface on the levels of cytokines and growth factors produced by oral keratinocytes Cal-27 was evaluated. The cytokines that significantly increased compared to the control after 24 and 48 h of co-culture were IL-1α, MCP-1 and IL-8; the latter two being chemoattractants consistent with the recruitment process of macrophages and neutrophils, respectively. IL-8 (CXCL8) plays an important role in the recruitment of neutrophils in the inflammatory phase and participates in angiogenesis, in addition to the processes of keratinocyte migration and cell proliferation. Several studies support that the keratinocyte expresses IL-8 during its proliferation [39]. On the other hand, Tonetti et al. [40] described the preferential location of IL-8 on the surface of the junctional epithelium. On the other hand, Tuschil et al. [39] showed that IL-8 increases the proliferation of keratinocytes from 10 % to 40 % compared to growth factors such as EGF. All this considering that IL-8 increases its expression in the phases of hemostasis, inflammation and cell proliferation [41].

MCP-1 (CCL2) is the major chemoattractant and activator of monocytes/macrophages; in mice, MCP-1 deficiency is associated with delays in angiogenesis, re-epithelialization, and collagen synthesis ([42] Low et al., 2001), suggesting that its role in tissue repair processes is essential. Gene expression results showed statistically significant overexpression of VEGF, FGF, TGF-β and EGF genes in co-cultures with biofunctionalized titanium surfaces compared to co-cultures with the control surface. The low levels ofIL-1β, IL-6, and TNF-α suggest that the biofunctionalized surface with laminin 332 does not induce a strong inflammatory response in oral keratinocytes that may favor tissue repair processes, which is supported by the high gene expression of TGF-β, EGF, VEGF, and FGF in co-cultured cells on these surfaces; In addition, the IL-8 and MCP-1 would play a key role in the proliferation of keratinocytes and the recruitment of M2 macrophages and fibroblasts for collagen synthesis thanks to the expression of FGF and TGF-β ([43] Terheyden et al., 2012). VEGF overexpression also plays a primary role in the angiogenesis process by supporting the high secretion of IL-8, which mediates this process. The results of this work allow us to conclude that the biofunctionalization of titanium surfaces (dental implant fragments) with laminin 332 promotes a tissue repair response profile in oral keratinocytes that can potentially favor the process of biological sealing, thereby helping to reduce the percentage of dental implant failures.

Contribution to the field statement

The study characterized the physical and chemical properties of the surfaces during the biofunctionalization process. The results showed that the Piranha solution treatment caused significant surface modifications, increasing the roughness and changing the surface morphology. These changes could lead to a more homogeneous distribution of silanes and proteins, affecting the amount of immobilized biomolecules on the titanium surface and thus influencing the cellular response. The surfaces functionalized with laminin 332 showed a similar Ra value as those treated with piranha solution; however, the Rq value did not change. In addition, the functionalized surfaces showed positive RSK, RKU, and RV values, indicating that the surface retained the morphology and roughness patterns formed by surface peaks. The work contributes to the field by providing insights into the mechanisms underlying the cellular response to biofunctionalized titanium dental implant surfaces, with implications for the development of new dental implant materials and techniques to enhance biological sealing.

Funding

This work has been supported by the vice-rectory of investigations of the Universidad El Bosque, Bogotá-Colombia.

Data availability statement

The data are included in article.

CRediT authorship contribution statement

Sandra J. Perdomo: Writing – review & editing, Writing – original draft, Supervision, Project administration, Methodology, Investigation, Funding acquisition, Formal analysis, Data curation, Conceptualization. **Carlos E. Fajardo:** Writing – original draft, Validation, Methodology, Investigation, Formal analysis, Data curation, Conceptualization. **Andrés Cardona-Mendoza:** Writing – review & editing, Writing – original draft, Supervision, Methodology, Investigation, Formal analysis, Conceptualization.

Declaration of competing interest

The authors declare the following financial interests/personal relationships which may be considered as potential competing interests: Sandra Janneth Perdomo Lara reports article publishing charges and equipment, drugs, or supplies were provided by University El Bosque. Sandra Janneth Perdomo Lara reports a relationship with University El Bosque that includes: employment. If there

are other authors, they declare that they have no known competing financial interests or personal relationships that could have appeared to influence the work reported in this paper.

Acknowledgments

The authors thank the Master of Dental Sciences and the Vice-Rector of Investigations of the University of El Bosque for their support and commitment in each process necessary to achieve this work successfully.

References

[1] P.I. Brånemark, U. Breine, R. Adell, B.O. Hansson, J. Lindström, A. Ohlsson, Intra osseous anchorage of dental prostheses: I. Experimental studies, Scand. J. Plast. ReConstr. Surg. Hand Surg. 3 (1969) 81–100, https://doi.org/10.3109/02844316909036699.
[2] W.L. Chai, I.M. Brook, A. Palmquist, R. Van Noort, K. Moharamzadeh, The biological seal of the implant-soft tissue interface evaluated in a tissueengineered oral mucosal model, J. R. Soc. Interface 9 (2012) 3528–3538, https://doi.org/10.1098/rsif.2012.0507.
[3] S.C.H. Yeung, Biological basis for soft tissue management in implant dentistry, Aust. Dent. J. 53 (2008) 39–42, https://doi.org/10.1111/j.1834-7819.2008.00040.x.
[4] S.E.A. Camargo, T. Roy, X. Xia, C. Fares, S.M. Hsu, F. Ren, A.E. Clark, D. Neal, J.F. Esquivel-Upshaw, Novel coatings to minimize corrosion of titanium in oral biofilm, Materials 14 (2) (2021) 342, https://doi.org/10.3390/ma14020342.
[5] S. Sakka, K. Baroudi, M.Z. Nassani, Factors associated with early and late failure of dental implants, J. Investig. Clin. Dent. 3 (2012) 258–261, https://doi.org/10.1111/j.2041-1626.2012.00162.x.
[6] E. Rompen, O. Domken, M. Degidi, A.E.P. Pontes, A. Piattelli, The effect of material characteristics, of surface topography and of implant components and connections on soft tissue integration: a literature review, Clin. Oral Implants Res. 17 (2006) 55–67, https://doi.org/10.1111/j.1600-0501.2006.01367.x.
[7] D.L. Cochran, J.S. Hermann, R.K. Schenk, F.L. Higginbottom, D. Buser, Biologic width around titanium implants. A histometric analysis of the implanto-gingival junction around unloaded and loaded nonsubmerged implants in the canine mandible, J. Periodontol. 68 (1997) 186–197, https://doi.org/10.1902/jop.1997.68.2.186.
[8] A. Nanci, D.D. Bosshardt, Structure of periodontal tissues in health and disease, Periodontol 40 (2000) 11–28, https://doi.org/10.1111/j.1600-0757.2005.00141.x, 2006.
[9] M. Hormia, K. Owaribe, I. Virtanen, The dento-epithelial junction: cell adhesion by type I hemidesmosomes in the absence of a true basal lamina, J. Periodontol. 72 (2001) 788–797, https://doi.org/10.1902/jop.2001.72.6.788.
[10] J. Oksanen, M. Hormia, I. Virtanen, M. Hormia, L.M. Sorokin, The junctional epithelium around murine teeth differs from gingival epithelium in its basement membrane composition, J. Dent. Res. 80 (2001) 2093–2097, https://doi.org/10.1177/00220345010800121401.
[11] T. Kinumatsu, S. Hashimoto, T. Muramatsu, H. Sasaki, H.S. Jung, S. Yamada, et al., Involvement of laminin and integrins in adhesion and migration of junctional epithelium cells, J. Periodontal. Res. 44 (2009) 13–20, https://doi.org/10.1111/j.1600-0765.2007.01036.x.
[12] H. Larjava, L. Koivisto, L. Häkkinen, J. Heino, Epithelial integrins with special reference to oral epithelia, J. Dent. Res. 90 (2011) 1367–1376, https://doi.org/10.1177/0022034511402207.
[13] M. Welander, I. Abrahamsson, T. Berglundh, The mucosal barrier at implant abutments of different materials, Clin. Oral Implants Res. 19 (7) (2008) 635–641, https://doi.org/10.1111/j.1600-0501.2008.01543.x.
[14] R. Glauser, P. Schüpbach, J. Gottlow, C.H.F. Hämmerle, Periimplant soft tissue barrier at experimental one-piece mini-implants with different surface topography in humans: a light-microscopic overview and histometric analysis, Clin. Implant Dent. Relat. Res. 7 (2005) s44–s51, https://doi.org/10.1111/j.1708-8208.2005.tb00074.x.
[15] M. Nevins, M.L. Nevins, M. Camelo, J.L. Boyesen, D.M. Kim, Human histologic evidence of a connective tissue attachment to a dental implant, Int. J. Periodontics Restor. Dent. 28 (2008) 111–121.
[16] R.N. Tamura, D. Oda, V. Quaranta, G. Plopper, R. Lambert, S. Glaser, et al., Coating of titanium alloy with soluble laminin-5 promotes cell attachment and hemidesmosome assembly in gingival epithelial cells: potential application to dental implants, J. Periodontal. Res. 32 (1997) 287–294, https://doi.org/10.1111/j.1600-0765.1997.tb00536.x.
[17] G.D. Marconi, L. Fonticoli, Y. Della Rocca, S. Oliva, T.S. Rajan, O. Trubiani, G. Murmura, F. Diomede, J. Pizzicannella, Enhanced extracellular matrix deposition on titanium implant surfaces: cellular and molecular evidences, Biomedicines 9 (11) (2021) 1710, https://doi.org/10.3390/biomedicines9111710.
[18] L. Tack, K. Schickle, F. Böke, H. Fischer, Immobilization of specific proteins to titanium surface using self-assembled monolayer technique, Dent. Mater. 31 (2015) 1169–1179, https://doi.org/10.1016/j.dental.2015.06.019.
[19] R.F. Abarca-Buis, E.A. Mandujano-Tinoco, A. Cabrera-Wrooman, E. Krötzsch, The complexity of TGFβ/activin signaling in regeneration, J. Cell Commun. Signal. 15 (2021) 7–23, https://doi.org/10.1007/s12079-021-00605-7.
[20] L. Guida, A. Oliva, M.A. Basile, M. Giordano, L. Nastri, M. Annunziata, Human gingival fibroblast functions are stimulated by oxidized nano-structured titanium surfaces, J. Dent. 41 (10) (2013) 900–907, https://doi.org/10.1016/j.jdent.2013.07.009.
[21] T. Berglundh, J. Lindhe, C. Marinello, I. Ericsson, B. Liljenberg, Soft tissue reaction to de novo plaque formation on implants and teeth. An experimental study in the dog, Clin. Oral Implants Res. 3 (1992) 1–8, https://doi.org/10.1034/j.1600-0501.1992.030101.x.
[22] Q. Jiang, Y. Yu, H. Ruan, Y. Luo, X. Guo, Morphological and functional characteristics of human gingival junctional epithelium, BMC Oral Health 14 (2014) 30, https://doi.org/10.1186/1472-6831-14-30.
[23] X. Wang, X. Huang, Y. Zhang, Involvement of human papillomaviruses in cervical cancer, Front. Microbiol. 9 (2018) 2896, https://doi.org/10.3389/fmicb.2018.02896.
[24] C.A. Middleton, C.J. Pendegrass, D. Gordon, J. Jacob, G.W. Blunn, Fibronectin silanized titanium alloy: a bioinductive and durable coating to enhance fibroblast attachment in vitro, J. Biomed. Mater. Res. 83 (2007) 1032–1038, https://doi.org/10.1002/jbm.a.31382.
[25] D.E. MacDonald, B.E. Rapuano, N. Deo, M. Stranick, P. Somasundaran, A.L. Boskey, Thermal and chemical modification of titanium-aluminum-vanadium implant materials: effects on surface properties, glycoprotein adsorption, and MG63 cell attachment, Biomaterials 25 (2004) 3135–3146, https://doi.org/10.1016/j.biomaterials.2003.10.029.
[26] L. Tack, K. Schickle, F. Böke, H. Fischer, Immobilization of specific proteins to titanium surface using self-assembled monolayer technique, Dent. Mater. 31 (2015) 1169–1179, https://doi.org/10.1016/j.dental.2015.06.019.
[27] L.D. Trino, E.S. Bronze-Uhle, A. Ramachandran, P.N. Lisboa-Filho, M.T. Mathew, A. George, Titanium surface bio-functionalization using osteogenic peptides: surface chemistry, biocompatibility, corrosion and tribocorrosion aspects, J. Mech. Behav. Biomed. Mater. 81 (2018) 26–38, https://doi.org/10.1016/j.jmbbm.2018.02.024.
[28] N. Mitik-Dineva, J. Wang, R.C. Mocanasu, P.R. Stoddart, R.J. Crawford, E.P. Ivanova, Impact of nano-topography on bacterial attachment, Biotechnol. J. 3 (2008) 536–544, https://doi.org/10.1002/biot.200700244.
[29] L. Le Guéhennec, A. Soueidan, P. Layrolle, Y. Amouriq, Surface treatments of titanium dental implants for rapid osseointegration, Dent. Mater. 23 (2007) 844–854, https://doi.org/10.1016/j.dental.2006.06.025.
[30] I.V. Panayotov, B.S. Vladimirov, P.-Y.C. Dutilleul, B. Levallois, F. Cuisinier, Strategies for immobilization of bioactive organic molecules on titanium implant surfaces - a review, Folia Med. 57 (2015) 11–18, https://doi.org/10.1515/folmed-2015-0014.

[31] M. Sedlaček, P. Gregorčič, B. Podgornik, Use of the roughness parameters Ssk and Sku to control friction—a method for designing surface texturing, Tribol. Trans. 60 (2017) 260–266, https://doi.org/10.1080/10402004.2016.1159358.
[32] R. Timpl, H. Rohde, P.G. Robey, S.I. Rennard, J.M. Foidart, G.R. Martin, Laminin–a glycoprotein from basement membranes, J. Biol. Chem. 254 (1979) 9933–9937.
[33] P.D. Yurchenco, E.C. Tsilibary, A.S. Charonis, H. Furthmayr, Laminin polymerization in vitro. Evidence for a two-step assembly with domain specificity, J. Biol. Chem. 260 (1985) 7636–7644.
[34] K.M. Woeppel, X.S. Zheng, X.T. Cui, Enhancing surface immobilization of bioactive molecules via a silica nanoparticle based coating, J. Mater. Chem. B 6 (2018) 3058–3067, https://doi.org/10.1039/C8TB00408K.
[35] H.-L. Graf, S. Stoeva, F.P. Armbruster, J. Neuhaus, H. Hilbig, Effect of bone sialoprotein and collagen coating on cell attachment to TICER® and pure titanium implant surfaces, Int. J. Oral Maxillofac. Surg. 37 (2008) 634–640, https://doi.org/10.1016/j.ijom.2008.01.021.
[36] J. Forsprecher, Z. Wang, H.A. Goldberg, M.T. Kaartinen, Transglutaminase-mediated oligomerization promotes osteoblast adhesive properties of osteopontin and bone sialoprotein, Cell Adhes. Migrat. 5 (2011) 65–72, https://doi.org/10.4161/cam.5.1.13369.
[37] I. Narimatsu, I. Atsuta, Y. Ayukawa, W. Oshiro, N. Yasunami, A. Furuhashi, et al., Epithelial and connective tissue sealing around titanium implants with various typical surface finishes, ACS Biomater. Sci. Eng. 5 (2019) 4976–4984, https://doi.org/10.1021/acsbiomaterials.9b00499.
[38] A. Baranowski, A. Klein, U. Ritz, A. Ackermann, J. Anthonissen, K.B. Kaufmann, et al., Surface functionalization of orthopedic titanium implants with bone sialoprotein, PLoS One 11 (2016) e0153978, https://doi.org/10.1371/journal.pone.0153978.
[39] H. Schliephake, D. Scharnweber, Chemical and biological functionalization of titanium for dental implants, J. Mater. Chem. 18 (2008) 2404–2414, https://doi.org/10.1039/B715355B.
[40] H. Ikeda, T. Yamaza, M. Yoshinari, Y. Ohsaki, Y. Ayukawa, M.A. Kido, T. Inoue, M. Shimono, K. Koyano, T. Tanaka, Estudios ultraestructurales y de microscopía inmunoelectrónica de la interfase epitelio-implante periimplantario (Ti-6Al-4V) del maxilar superior de rata, Revista de Periodoncia 71 (6) (2000) 961–973, https://doi.org/10.1902/jop.2000.71.6.961.
[41] V.P. Koidou, P.P. Argyris, E.P. Skoe, J. Mota Siqueira, X. Chen, L. Zhang, J.E. Hinrichs, M. Costalonga, C. Aparicio, Los recubrimientos peptídicos mejoran la unión de los queratinocitos para mejorar el sellado de la mucosa periimplantaria, Ciencia de los Biomater. 6 (7) (2018) 1936–1945, https://doi.org/10.1039/c8bm00300a.
[42] A. Tuschil, C. Lam, A. Haslberger, I. Lindley, Interleukin-8 stimulates calcium transients and promotes epidermal cell proliferation, J. Invest. Dermatol. 99 (1992) 294–298, https://doi.org/10.1111/1523-1747.ep12616634.
[43] M.S. Tonetti, Determination of the success and failure of root-form osseointegrated dental implants, Adv. Dent. Res. 13 (1999) 173–180, https://doi.org/10.1177/08959374990130010801.